

# Quantum Cryptography using entangled photons in energy-time Bell states

W. Tittel, J. Brendel, H. Zbinden, and N. Gisin

*Group of Applied Physics, University of Geneva, CH-1211, Geneva 4, Switzerland*

We present a setup for quantum cryptography based on photon pairs in energy-time Bell states and show its feasibility in a laboratory experiment. Our scheme combines the advantages of using photon pairs instead of faint laser pulses and the possibility to preserve energy-time entanglement over long distances. Moreover, using 4-dimensional energy-time states, no fast random change of bases is required in our setup: Nature itself decides whether to measure in the energy or in the time base.

PACS Nos. 3.67.Dd, 3.67.Hk

Quantum communication is probably one of the most rapidly growing and most exciting fields of physics within the last years [1]. Its most mature application is quantum cryptography (also called quantum key distribution), ensuring the distribution of a secret key between two parties. This key can be used afterwards to encrypt and decrypt secret messages using the one time pad [2]. In opposition to the mostly used "public key" systems [2], the security of quantum cryptography is not based on mathematical complexity but on an inherent property of single quanta. Roughly speaking, since it is not possible to measure an unknown quantum system without modifying it, an eavesdropper manifests herself by introducing errors in the transmitted data. During the last years, several prototypes based on faint laser pulses mimicking single photons, have been developed, demonstrating that quantum cryptography not only works inside the laboratory, but in the "real world" as well [1,3,4]. Besides, it has been shown that two-photon entanglement can be preserved over large distances [5], especially when being entangled in energy and time [6]. As pointed out by Ekert in 1991 [7], the nonlocal correlations engendered by such states can also be used to establish sequences of correlated bits at distant places, the advantage compared to systems based on faint laser pulses being the smaller vulnerability against a certain kind of eavesdropper attack [8,9].

Besides improvements in the domain of quantum key distribution, recent experimental progress in generating, manipulating and measuring the so-called Bell-states [10], has led to fascinating applications like quantum teleportation [11], dense-coding [12] and entanglement swapping [13]. In a recent paper, we proposed and tested a novel source for quantum communication generating a new kind of Bell states based on energy-time entanglement [14]. In this paper, we present a first application, exploiting this new source for quantum cryptography. Our scheme follows Ekert's initial idea concerning the use of photon-pair correlations. However, in opposition, it implements Bell states and can thus be seen in the

broader context of quantum communication. Moreover, the fact that energy-time entanglement can be preserved over long distances renders our source particularly interesting for long-distance applications.

To understand the principle of our idea, we look at Fig. 1. A short light pulse emitted at time  $t_0$  enters an interferometer having a path length difference which is large compared to the duration of the pulse. The pulse is thus split into two pulses of smaller amplitudes, following each other with a fixed phase relation. The light is then focussed into a nonlinear crystal where some of the pump photons are downconverted into photon pairs. Working with pump energies low enough to ensure that generation of two photon pairs by the same as well as by two subsequent pulses can be neglected, a created photon pair is described by

$$|\psi\rangle = \frac{1}{\sqrt{2}} \left( |s\rangle_A |s\rangle_B + e^{i\phi} |l\rangle_A |l\rangle_B \right). \quad (1)$$

$|s\rangle$  and  $|l\rangle$  denote a photon created by a pump photon having traveled via the short or the long arm of the interferometer, and the indices A, B label the photons. The state (1) is composed of only two discrete emission times and not of a continuous spectrum. This contrasts with the energy-time entangled states used up to now [7,15]. Please note that, depending on the phase  $\phi$ , Eq. (1) describes two of the four Bell states. Interchanging  $|s\rangle$  and  $|l\rangle$  for one of the two photons leads to generation of the remaining two Bell-states. In general, the coefficients describing the amplitudes of the  $|s\rangle|s\rangle$  and  $|l\rangle|l\rangle$  states can be different, leading to nonmaximally entangled states. However, in this article, we will deal only with maximally entangled states. Behind the crystal, the photons are separated and are sent to Alice and Bob, respectively (see Fig.1). There, each photon travels via another interferometer, introducing exactly the same difference of travel times through one or the other arm as did the previous interferometer, acting on the pump pulse. If Alice looks at the arrival times of the photons with respect to the emission time of the pump pulse  $t_0$  – note that she has two detectors to look at –, she will find the photons in one of three time slots. For instance, detection of a photon in the first slot corresponds to "pump photon having traveled via the short arm and downconverted photon via the short arm". To keep it short, we refer to this process as  $|s\rangle_P; |s\rangle_A$ , where  $P$  stands for the pump- and  $A$  for Alice's photon. However, the characterization of the complete photon pair is still ambiguous, since, at this point, the path of the photon having traveled to Bob (short or long in his interferometer) is unknown to Alice. Fig. 1 illustrates all processes

leading to a detection in the different time slots both at Alice's and at Bob's detector. Obviously, this reasoning holds for any combination of two detectors. In order to build up the secret key, Alice and Bob now publicly agree about the events where both detected a photon in one of the satellite peaks – without revealing in which one – or both in the central peak – without revealing the detector. This additional information enables both of them to know exactly via which arm the sister photon, detected by the other person, has traveled. For instance, to come back to the above given example, if Bob tells Alice that he detected his photon in a satellite peak as well, she knows that the process must have been  $|s\rangle_p; |s\rangle_A |s\rangle_B$ . The same holds for Bob who now knows that Alice photon traveled via the short arm in her interferometer. If both find the photons in the right peak, the process was  $|l\rangle_p; |l\rangle_A |l\rangle_B$ . In either case, Alice and Bob have correlated detection times. The cross terms where one of them detect a photon in the left and the other one in the right satellite peak do not occur. Assigning now bitvalues 0 (1) to the short (long) processes, Alice and Bob finally end up with a sequence of correlated bits.

Otherwise, if both find the photon in the central slot, the process must have been  $|s\rangle_p; |l\rangle_A |l\rangle_B$  or  $|l\rangle_p; |s\rangle_A |s\rangle_B$ . If both possibilities are indistinguishable, we face the situation of interference and the probability for detection by a given combination of detectors (e.g. the "+"-labeled detector at Alice's and the "-" labeled one at Bob's) depends on the phases  $\alpha$ ,  $\beta$  and  $\phi$  in the three interferometers. The quantum mechanical treatment leads to  $P_{i,j} = \frac{1}{2}(1 + ij\cos(\alpha + \beta - \phi))$  with  $i, j = \pm 1$  denoting the detector labels [14]. Hence, choosing appropriate phase settings, Alice and Bob will always find perfect correlations in the output ports. Either both detect the photons in detector "-" (bitvalue "0"), or both in detector "+" (bitvalue "1"). Since the correlations depend on the phases and thus on the energy of the pump, signal and idler photons, we refer to this base as the energy base (showing wave like behaviour), stressing the complementarity with the other, the time basis (showing particle like behaviour).

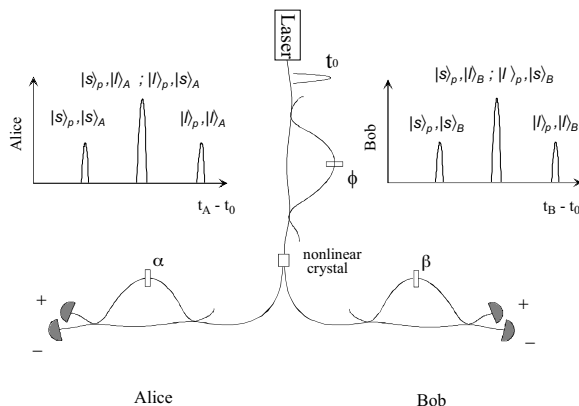


FIG. 1. Schematics of quantum key distribution using energy-time Bell states.

Like in the BB84 protocol [16] it is the use of complementary bases that ensures the detection of an eavesdropper [17]. If we consider for instance the most intuitive intercept/resend strategy, the eavesdropper intercepts the photons, measures them in one of the two bases and sends new, accordingly prepared photons instead. Since she never knows in which basis Bob's measurement will take place, she will in half of the cases eavesdrop and resend the photons in the "wrong basis" and therefore will statistically introduce errors in Bob's results, revealing in turn her presence. For a more general treatment of quantum key distribution and eavesdropping using energy-time complementarity, we refer the reader to [18].

To generate the short pump pulses, we use a pulsed diode laser (PicoQuant PDL 800), emitting 600ps (FWHM) pulses of 655 nm wavelength at a repetition frequency of 80 MHz. The average power is of  $\approx 10$  mW, equivalent to an energy of 125 pJ per pulse. The light passes a dispersive prism, preventing the small quantity of also emitted infrared light to enter the subsequent setup, and a polarizing beamsplitter (PBS), serving as optical isolator. The pump is then focussed into a single-mode fiber and is guided into a fiber optical Michelson interferometer made of a 3 dB fiber coupler and chemically deposited silver end mirrors. The path length difference corresponds to a difference of travel times of  $\approx 1.2$  ns, splitting the pump pulse into two, well separated pulses. The arm-length difference of the whole interferometer can be controlled using a piezoelectric actuator in order to ensure any desired phase difference. Besides, the temperature is maintained stable. In order to control the evolution of the polarization in the fibers, we implement three fiber-optical polarization controllers, each one consisting of three inclinable fiber loops – equivalent to three waveplates in the case of bulk optic. The first device is placed before the interferometer and ensures that all light, leaving the Michelson interferometer by the input port will be reflected by the already mentioned PBS and thus will not impinge onto the laser diode. The second controller serves to equalize the evolution of the polarization states within the different arms of the interferometer, and the last one enables to control the polarization state of the light that leaves the interferometer by the second output port. The horizontally polarized light is now focussed into a 4x3x12 mm  $KNbO_3$  crystal, cut and oriented to ensure degenerate collinear phase-matching, hence producing photon pairs at 1310 nm wavelength – within the so-called second telecommunication window. Due to injection losses of the pump into the fiber and losses within the interferometer, the average power before the crystal drops to  $\approx 1$  mW, and the energy per pulse – remember that each initial pump pulse is now split into two – to  $\approx 6$  pJ. The probability for creation of more than one photon pair within the same or within two subsequent pulses is smaller than 1 %, ensuring the assumption that lead to Eq. 1. Behind the crystal, the red pump light is absorbed by a filter (RG 1000). The down-

converted photons are then focussed into a fiber coupler, separating them in half of the cases, and are guided to Alice and Bob, respectively. The interferometers (type Michelson) located there have been described in detail in [6]. They consist of a 3-port optical circulator, providing access to the second output arm of the interferometer, a 3 dB fiber coupler and Faraday mirrors in order to compensate any birefringence within the fiber arms. To control their phases, the temperature can be varied or can be maintained stable. Overall losses are about 6 dB. The path length differences of both interferometers are equal with respect to the coherence length of the down-converted photons – approximately  $20 \mu\text{m}$ . In addition, the travel time difference is the same than the one introduced by the interferometer acting on the pump pulse. In this case, "the same" refers to the coherence time of the pump photons, around 800 fs or 0.23 mm, respectively.

To detect the photons, the output ports are connected to single-photon counters – passively quenched germanium avalanche photodiodes, operated in Geiger-mode and cooled to 77 K [6]. We operate them at dark count rates of 30 kHz, leading to quantum efficiencies of  $\approx 5\%$ . The single photon detection rates are of 4-7 kHz, the discrepancy being due to different detection efficiencies and losses in the circulators. The signals from the detectors as well as signals being coincident with the emission of a pump pulse are fed into fast AND-gates.

To demonstrate our scheme, we first measure the correlated events in the time base. Conditioning the detection at Alice's and Bob's detectors both on the left satellite peaks, ( $|s_p\rangle, |s_A\rangle$ ) and ( $|s_p\rangle, |s_B\rangle$ ), respectively) we count the number of coincident detections between both AND-gates, that is the number of triple coincidences between emission of the pump-pulse and detections at Alice's and Bob's. In subsequent runs, we measure these rates for the right-right ( $|l_p\rangle, |l_A\rangle$  AND  $|l_p\rangle, |l_B\rangle$ ) events, as well as for the right-left cross terms. We find values around 1700 coincidences per 100 sec for the correlated, and around 80 coincidences for the non-correlated events (table 1). From the four times four rates –remember that we have four pairs of detectors–, we calculate the different quantum bit error rates QBER, which is the ratio of wrong to detected events. We find values inbetween 3.7 and 5.7 %, leading to a mean value of QBER for the time base of  $(4.6 \pm 0.1)\%$ .

In order to evaluate the QBER in the energy base, we condition the detection at Alice's and Bob's on the central peaks. Changing the phases in any of the three interferometers, we observe interference fringes in the triple coincidence count rates (Fig.2). Fits yield visibilities of 89.3 to 94.5 % for the different detector pairs (table 2). In the case of appropriately chosen phases, the number of correlated events are around 800 in 50 sec, and the number of errors are around 35. From these values, we calculate the QBERs for the four detector pairs. We find values inbetween 2.8 and 5.4 %, leading to a mean QBER for the energy base of  $(3.9 \pm 0.4)\%$ . Note that this experiment can be seen as a Franson-type test of

Bell inequalities as well [15,19]. From the mean visibility of  $(92.2 \pm 0.8)\%$ , we can infer to a violation of Bell inequalities by 27 standard deviations.

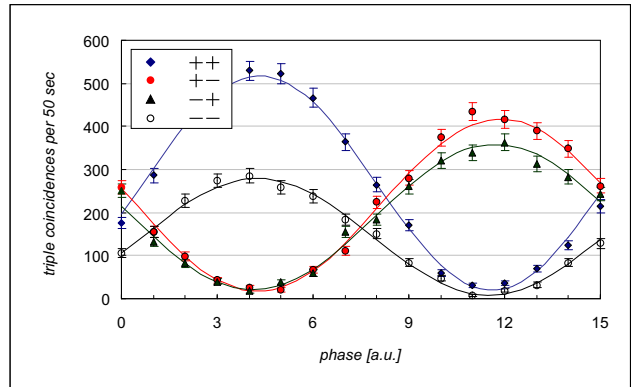


FIG. 2. Results of the measurement in the energy basis. The different mean values are due to different detector efficiencies

Like in all experimental quantum key distribution schemes, the found QBERs are non-zero, even in the absence of any eavesdropping. Nevertheless, they are still small enough to guarantee the detection of an eavesdropper attack, allowing thus secure key distribution. inequality The remaining  $\approx 4\%$  are due to accidental coincidences from uncorrelated events at the single photon detectors, a not perfectly localized pump pulse, non-perfect time resolution of the photon detectors, and, in the case of the energy basis, non-perfect interference. Note that the last mentioned errors decrease at the same rate as the number of correlated events when increasing the distance between Alice and Bob (that is when increasing the losses). In contrast to that, the number of errors due to uncorrelated events (point 1) stays almost constant since it is dominated by the detector noise. Thus, the QBER increases with distance, however, only at a small rate since this contribution was found to be small. Experimental investigations show that introducing 6 dB overall losses – in the best case equivalent to 20 km of optical fiber – leads to an increment of only around 1%, hence to a QBER of 5-6%. Besides detector noise, another major problem of all quantum key distribution schemes developed up to now is stability, the only exception being [3]. In order to really implement our setup for quantum cryptography, the interferometers have to be actively stabilized, taking for instance advantage of the free ports. The chosen passive stabilization by controlling the temperature is not sufficient to ensure stable phases over a long time.

To conclude, we presented a new setup for quantum cryptography using Bell states based on energy-time entanglement, and demonstrated its feasibility in a laboratory experiment. We found bit rates of around 33 Hz and quantum bit error rates of around 4 % which is low enough to ensure secure key distribution. Besides a smaller vulnerability against eavesdropper attacks, the

advantage of using discrete energy-time states, up to dimension 4, in our scheme, is the fact that no fast change between non-commuting bases is necessary. Nature itself chooses between the complementary properties energy and time. Furthermore, the recent demonstration that energy-time entanglement can be preserved over long distances [6] shows that this scheme is perfectly adapted to long-distance quantum cryptography.

We would like to thank J.D. Gautier for technical support and PicoQuant for fast delivery of the laser. This work was supported by the Swiss PPOII and the European QuCom IST projects.

- 
- [1] Physics World, March 1998, special issue in quantum communication including an article by W. Tittel, G. Ribordy, and N. Gisin on quantum cryptography.
- [2] See e.g. D. Welsh, Codes and Cryptography, Oxford Science Publication, Clarendon Press, Oxford (1988).
- [3] A. Muller, T. Herzog, B. Huttner, W. Tittel, H. Zbinden, and N. Gisin, Appl. Phys. Lett **70**, 793 (1997). G. Ribordy, J.-D. Gautier, N. Gisin, O. Guinnard, and H. Zbinden. quant-ph/9905056.
- [4] P.D. Townsend. Opt. Fiber Technology **4**, 345 (1998). R.J. Hughes, G.L. Morgan, and C.G. Peterson. quant-ph/9904038. J.-M. Mérola, Y. Mazurenko, J.-P. Goedgebuer, and W.T. Rhodes. Phys. Rev. Lett. **82**, 1656 (1999).
- [5] P.R. Tapster, J.G. Rarity, and P.C.M. Owens. Phys. Rev. Lett. **73**, 1923 (1994). W. Tittel, J. Brendel, N. Gisin, T. Herzog, and H. Zbinden. Phys. Rev. A **57**, 3229 (1998). W. Tittel, J. Brendel, H. Zbinden, and N. Gisin. Phys. Rev. Lett. **81**, 3563 (1998). G. Weihs, T. Jennewein, C. Simon, H. Weinfurter, and A. Zeilinger, Phys. Rev. Lett. **81**, 5039 (1998).
- [6] W. Tittel, J. Brendel, N. Gisin, and H. Zbinden. Phys. Rev. A **59**, 4150 (1999).
- [7] A.K. Ekert, Phys. Rev. Lett. **67**, 661 (1991).
- [8] When using coherent states, the eavesdropper can take advantage of the fact that there always is a small probability of finding more than one photon in the same pulse, hence in the same state. In these cases, she simply measures one and lets pass the other one unmeasured. This strategy can be somewhat circumvented using photon pairs, where one photon serves as trigger for the second one. However, since the possibility to create more than one pair at the same time increases with the pump intensity, we face a similar problem concerning the simultaneous presence of more than one photon in the same state. Note that this probability can be made arbitrarily small in both cases using weaker pulses or lower pump energies. Still, there is an important difference, favouring the implementation of photon pairs: Whenever the trigger photon has been detected, there is one photon left in the setup. This contrasts with the schemes based on faint

pulses where the detecting electronics has to be activated whenever a weak pulse (containing most of the time no photon) was emitted.

- [9] G. Brassard, N. Lütkenhaus, T. Mor, and B.C. Sanders. quant-ph/9911054.
- [10] H. Weinfurter, Europhys. Lett **25**, 559 (1994). M. Michler, K. Mattle, H. Weinfurter, and A. Zeilinger. Phys. Rev. A **53**, R1209 (1996).
- [11] C.H. Bennett, G. Brassard, C. Crpeau, R. Jozsa, A. Peres, and W.K. Wootters. Phys. Rev. Lett. **70** 1895 (1993). D. Bouwmeester, J.-W. Pan, K. Mattle, M. Eibl, D. Boschi, S. Branca, F. De Martini, L. Hardy, and S. Popescu. Phys. Rev. Lett. **80**, 1121 (1998). A. Furusawa, J.L. Sorensen, S.L. Braunstein, C.A. Fuchs, H.J. Kimble, and E.S. Polzik. Science **282**, 706 (1998).
- [12] K. Mattle, H. Weinfurter, P.G. Kwiat, and A. Zeilinger. Phys. Rev. Lett. **76**, 4656 (1996).
- [13] J.-W. Pan, D. Bouwmeester, H. Weinfurter, and A. Zeilinger. Phys. Rev. Lett. **80**, 3891 (1998).
- [14] J. Brendel, N. Gisin, W. Tittel, and H. Zbinden. Phys. Rev. Lett. **82**, 2594 (1999).
- [15] J.D. Franson, Phys. Rev. Lett. **62**, 2205 (1989).
- [16] C.H. Bennett and G. Brassard, in Proceedings of IEEE International Conference on Computers, Systems and Signal Processing, Bangalore, India (IEEE, New York, 1984), p.175
- [17] C. Fuchs, N. Gisin, R. B. Griffiths, C. S. Niu and A. Peres Phys. Rev. A **56**, 1163 (1997). I. Cirac and N. Gisin, Phys. Lett. A **229**, 1 (1997).
- [18] H. Bechmann-Pasquinucci and W. Tittel. quant-ph/9910095.
- [19] J.S. Bell, Physics **1**, 195 (1964).

	++	+-	-+	--
$s_{PSA} \& s_{PSB}$	278±6	197±5	187±5	147±4
$l_{PLA} \& l_{PLB}$	304±7	201±5	200±5	148±5
$s_{PSA} \& l_{PLB}$	11±0.8	10.4±0.8	9.2±0.7	9.4±0.7
$l_{PLA} \& s_{PSB}$	11.2±0.4	8.6±0.4	9.1±0.4	8.5±0.4
QBER [%]	3.7±0.2	4.6±0.2	4.5±0.2	5.7±0.3

TABLE I. Results of the measurement in the time basis. The different coincidence count rates are due to different quantum efficiencies of the detectors, and the slight asymmetry in the correlated events can be explained by the non-equal transmission probabilities within the interferometers.

	++	+-	-+	--
Visibility [%]	92.5±1.8	92.6±1.4	89.3±1.9	94.5±1.6
max.	518±13	416±8	359±9	279±7
min.	20±5	16±3	20±4	8±2
QBER [%]	3.7±0.9	3.7±0.7	5.3±1	2.8±0.8

TABLE II. Results of the measurement in the energy-basis.